Acoustic eigenvalues of rectangular rooms with arbitrary wall impedances using the interval Newton/generalized bisection method

Yusuke Naka[a)]
Department of Aerospace and Mechanical Engineering, Boston University, 677 Beacon Street, Boston, Massachusetts 02215

Assad A. Oberai
Department of Aerospace and Mechanical Engineering, Boston University, 110 Cummington Street, Boston, Massachusetts 02215

Barbara G. Shinn-Cunningham
Boston University Hearing Research Center, 677 Beacon Street, Boston, Massachusetts 02215

(Received 23 May 2005; revised 13 September 2005; accepted 15 September 2005)

Modal analysis of a rectangular room requires evaluation of the eigenvalues of the Helmholtz operator while taking into account the boundary conditions imposed on the walls of the room. When the walls have finite impedances, the acoustic eigenvalue equation becomes complicated and a numerical method that can find all roots within a given interval is required to solve it. In this study, the interval Newton/generalized bisection (IN/GB) method is adopted for solving this problem. For an efficient implementation of this method, bounds are derived for the acoustic eigenvalues and their asymptotic behavior explored. The accuracy of the IN/GB method is verified for a canonical problem by comparing the modal solution with the corresponding finite element solution. Furthermore, reverberation times estimated using the IN/GB method are compared to those calculated using the finite difference method. Through these examples, it is demonstrated that the IN/GB method provides a useful and efficient approach for estimating the acoustic responses of rectangular rooms with finite wall impedances. © *2005 Acoustical Society of America.* [DOI: 10.1121/1.2114607]

PACS number(s): 43.55.Br, 43.55.Ka, 43.20.Ks [NX] Pages: 3662–3671

I. INTRODUCTION

Modal analysis is a classical method for solving problems in room acoustics (see, for example, Refs. 1–5). Using this method, once all the normal modes are known, the acoustic pressure distribution for an arbitrary sound source in a room can be easily computed. Although the modal theory of room acoustics was established and fully formulated over a half century ago,[1] it is still incomplete in the sense that there is no well-developed, general method for finding eigenvalues that correspond to room modes for walls with arbitrary impedances. Only for rooms with perfectly or nearly rigid walls or rooms with the same impedance on each pair of parallel walls are the eigenvalues or their approximations easy to evaluate. Hence, only these cases have typically been considered in the acoustics literature.[1–6] However, the effect of finite wall impedances on quantities of interest, such as the reverberation time, is of general interest and important for real-world problems. Hence there is a need for an efficient and accurate method for evaluating eigenvalues for the more general case.

The difficulty in finding the acoustic eigenvalues arises from the nonlinear and transcendent nature of the acoustic eigenvalue equation,[1,2,5] which necessitates the use of numerical methods. In addition, for the modal solution to be accurate, these methods must be able to evaluate all the roots of this equation within a given interval. Classical numerical approaches for solving nonlinear equations such as Newton's iteration are not suitable for solving these equations because they yield one root for a single initial guess. Moreover, the initial guess must be "good" in order to obtain a root in the range of interest. If the number of roots in a range of interest is unknown, which is often the case in the acoustic eigenvalue problem for a room with finite wall impedances, these methods cannot be applied. Although several numerical methods have been developed to attack this problem (some of which work relatively well),[7,8] it is generally recognized that a simpler, more efficient, and stabler method would greatly increase the practicality of using modal analysis in studies of room acoustics.

In this study, the interval Newton/generalized bisection (IN/GB) method[9–11] is applied to the acoustic eigenvalue equation to overcome the above-mentioned difficulties. The IN/GB method is an extension of the classical Newton iterative method, combined with the concept of interval arithmetic.[9–12] The method is guaranteed to find all possible solutions of a system of equations within intervals specified for each variable. In addition, the quadratic convergence of the Newton method is preserved.[11]

[a)]Corresponding Author; Electronic mail: ynaka@bu.edu

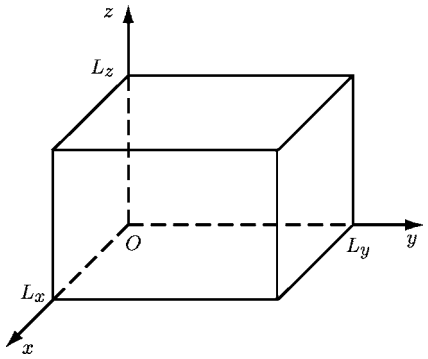

FIG. 1. Coordinate system of a rectangular room.

The remainder of this paper is organized as follows. In Sec. II, we derive the acoustic eigenvalue equation. In Sec. III, we discuss the application of the IN/GB method to the acoustic eigenvalue problem. In particular, we derive limits and approximations of eigenvalues that yield "good" initial guesses for intervals used in this method. These limits and approximations are useful not only for efficient implementation of the IN/GB method, but find more general applications. The subsequent sections describe three numerical experiments. In Sec. IV, we evaluate acoustic eigenvalues using the IN/GB method for a one-dimensional problem. In Sec. V, we evaluate the modal solution for a point source problem and compare our results with a benchmark solution obtained using the finite element method (FEM). In Sec. VI, we estimate room reverberation times using the acoustic eigenvalues, and compare our results with calculations using the finite-difference time-domain (FDTD) method.[13] We make concluding remarks in Sec. VII. In the Appendices, we review interval arithmetic first, and then describe the IN/BG method for single and multiple variable problems, of which the latter is required for solving the acoustic eigenvalue equation.

II. ACOUSTIC EIGENVALUE EQUATIONS

Normal modes of a rectangular room are obtained by solving the homogeneous Helmholtz (reduced wave) equation. For a room with uniform impedance on each of its walls, the three-dimensional homogeneous Helmholtz problem for the acoustic pressure $p(x,y,z)$ is described as

$$-\nabla^2 p - k^2 p = 0, \quad \text{in } \Omega, \tag{1}$$

$$\nabla p \cdot \mathbf{n} = -i\frac{\rho c}{Z_j} kp = -i\eta_j kp, \quad \text{on } \Gamma_j, \tag{2}$$

where Ω is the entire space of the room, Γ_j is the jth wall whose impedance is denoted by Z_j, i is the imaginary unit, $k=\omega/c$ is the driving wave number with angular frequency ω, c is the speed of sound, $\mathbf{n}$ is the outward normal unit vector on the walls, ρ is the density of the medium inside the room, and $\eta_j=\rho c/Z_j$ are the specific acoustic admittances of the walls. Figure 1 shows the coordinate system used for this problem. The domain is $\Omega=(0,L_x)\times(0,L_y)\times(0,L_z)$.

The solution of this homogeneous Helmholtz problem can be obtained by the separation of variables.[1–5] Exponentials are chosen as the eigenfunctions in this study; for example, the eigenfunction in the x direction is given in the form

$$\phi_x(x) = Ae^{ik_x x} + Be^{-ik_x x}, \tag{3}$$

where k_x (which is generally a complex value) is the eigenvalue in the x direction, and A and B are complex constants. After applying Eq. (3) to the boundary conditions Eqs. (2) at $x=0$ and $x=L_x$, the lth eigenfunction in the x direction is obtained as

$$\phi_{xl}(x) = (k_{xl} + \eta_1 k)e^{ik_{xl}x} + (k_{xl} - \eta_1 k)e^{-ik_{xl}x}, \tag{4}$$

where η_1 is the specific acoustic admittance at $x=0$. k_{xl} is the lth root of k_x for the following acoustic eigenvalue equation:

$$e^{i2k_x L_x} = \frac{(k_x - \eta_1 k)(k_x - \eta_2 k)}{(k_x + \eta_1 k)(k_x + \eta_2 k)}, \tag{5}$$

in which η_2 is the specific acoustic admittance at $x=L_x$. The eigenfunctions and eigenvalues in the y and z directions can be defined in the similar manner.

Since Eq. (5) is a nonlinear equation involving exponentials, its analytical solution is not feasible. Hence, it must be solved numerically, using a method that will yield all roots in a given interval. The solution of this problem using standard Newton's iteration with several initial guesses is fraught with difficulties, as different guesses might lead to the same root and it is impossible to determine if all roots within an interval have been estimated.

With this as motivation, the applicability of the IN/GB method for solving this problem is explored. The IN/GB method evaluates all possible solutions of a nonlinear equation system within a given range, and is therefore an appropriate method for finding all important eigenvalues of the acoustic eigenvalue equation. Interval arithmetic and the IN/GB method are reviewed in the Appendices. For a more detailed analysis of this method, the reader is referred to Refs. 9–12.

III. APPLICATION OF IN/GB METHOD TO ACOUSTIC EIGENVALUE EQUATIONS

A. Formulation of acoustic eigenvalue equation for IN/GB method

The IN/GB method is defined for real intervals (see the Appendices). However, the approach can be used to find complex roots in the acoustic eigenvalue equation, Eq. (5), by splitting the complex values into real and imaginary parts. Two separate equations derived from the real and imaginary components can then be written as $f_1(k_{xR},k_{xI})=0$ and $f_2(k_{xR},k_{xI})=0$, respectively. In this study, the following form is considered:

$$
\begin{aligned}
&f_1(k_{xR},k_{xI})\\
&\quad\equiv (k_{xR}-\eta_{1R}k)(k_{xR}-\eta_{2R}k)-(k_{xI}-\eta_{1I}k)(k_{xI}-\eta_{2I}k)\\
&\quad\quad -e^{-2k_{xI}L_x}\{\cos(2k_{xR}L_x)[(k_{xR}+\eta_{1R}k)(k_{xR}+\eta_{2R}k)\\
&\quad\quad -(k_{xI}+\eta_{1I}k)(k_{xI}+\eta_{2I}k)]-\sin(2k_{xR}L_x)[(k_{xR}+\eta_{1R}k)\\
&\quad\quad \times(k_{xI}+\eta_{2I}k)+(k_{xI}+\eta_{1I}k)(k_{xR}+\eta_{2R}k)]\}=0, \qquad (6)
\end{aligned}
$$

$$
\begin{aligned}
&f_2(k_{xR},k_{xI})\\
&\quad\equiv (k_{xR}-\eta_{1R}k)(k_{xI}-\eta_{2I}k)+(k_{xI}-\eta_{1I}k)(k_{xR}-\eta_{2R}k)\\
&\quad\quad -\{\cos(2k_{xR}L_x)[(k_{xR}+\eta_{1R}k)(k_{xI}+\eta_{2I}k)\\
&\quad\quad +(k_{xI}+\eta_{1I}k)(k_{xR}+\eta_{2R}k)]+\sin(2k_{xR}L_x)[(k_{xR}+\eta_{1R}k)\\
&\quad\quad \times(k_{xR}+\eta_{2R}k)-(k_{xI}+\eta_{1I}k)(k_{xI}+\eta_{2I}k)]\}=0. \qquad (7)
\end{aligned}
$$

The subscripts R and I denote the real and imaginary parts, respectively. Equations (6) and (7) are solved for k_{xR} and k_{xI} using the multivariate IN/GB method.

B. Limits and approximations of acoustic eigenvalues

Although the IN/GB method is guaranteed to find all roots in a given interval, an intelligent choice of the initial intervals makes it more efficient. In this section, the limits and the asymptotic behavior of the acoustic eigenvalues are derived in three theorems. Taken together, these three theorems significantly reduce the size of the initial intervals (from the entire complex plane).

Theorem 1: *The solutions of the acoustic eigenvalue equation appear in pairs of opposite signs.*

Proof: Replacing k_x by $-k_x$ in the acoustic eigenvalue equation, Eq. (5) leads to the same equation. Hence, if $\hat{k}_x$ is a solution of Eq. (5), then $-\hat{k}_x$ also satisfies this equation. ■

This theorem illustrates that it is sufficient to find solutions in only half of the complex plane. In this study, $k_{xI}\geqslant 0$ is considered. In this half-plane, $0<e^{-2k_{xI}L_x}\leqslant 1$ in Eqs. (6) and (7), while on the other half of the plane, it grows to infinity as k_{xI} decreases. For this reason, solutions are sought, even for $k_{xR}\leqslant 0$, although nonpositive values of k_{xR} are of no interest from a physical point of view. If a root with negative real part is found, then the root that has the opposite sign is an eigenvalue of interest.

While the lower limit of k_{xI} is determined from Theorem 1, the next theorem indicates that k_{xI} cannot be infinite. Taken together, these two theorems show that the interval to be searched for the imaginary parts of roots can be restricted to a moderate range.

Theorem 2: *Let $\hat{k}_{xR}$ and $\hat{k}_{xI}$ be the real and imaginary parts of a root of the acoustic eigenvalue equation, respectively. If $\hat{k}_{xI}\geqslant 0$, then $\hat{k}_{xI}$ is not much larger than* $\max\{1/2L_x,|\eta_1 k|,|\eta_2 k|\}$.

Proof: Let ε be a real number such that $|\varepsilon|\ll 1$. If $\hat{k}_{xI}\gg 1/2L_x,|\eta_1 k|,|\eta_2 k|$, then $e^{-2\hat{k}_{xI}L_x}$, $\eta_{1R}k/\hat{k}_{xI}$, $\eta_{1I}k/\hat{k}_{xI}$, $\eta_{2R}k/\hat{k}_{xI}$, and $\eta_{2I}k/\hat{k}_{xI}$ can be represented in terms of ε as $e^{-1/(a_e\varepsilon)}$, $a_{1R}\varepsilon$, $a_{1I}\varepsilon$, $a_{2R}\varepsilon$, and $a_{2I}\varepsilon$, respectively, where a's satisfy $|a|\leqslant 1$. Dividing Eqs. (6) and (7) by $\hat{k}_{xI}^2$ and denoting $\hat{k}_{xR}/\hat{k}_{xI}$ by ρ gives

$$
\begin{aligned}
&(\rho-a_{1R}\varepsilon)(\rho-\alpha_{2R}\varepsilon)-(1-a_{1I}\varepsilon)(1-a_{2I}\varepsilon)\\
&\quad=e^{-1/(a_e\varepsilon)}\{\cos(2\hat{k}_{xR}L_x)[(\rho+a_{1R}\varepsilon)(\rho+a_{2R}\varepsilon)\\
&\quad\quad -(1+a_{1I}\varepsilon)(1+a_{2I}\varepsilon)]\\
&\quad\quad -\sin(2\hat{k}_{xR}L_x)[(\rho+a_{1R}\varepsilon)(1+a_{2I}\varepsilon)\\
&\quad\quad +(1+a_{1I}\varepsilon)(\rho+a_{2R}\varepsilon)]\}, \qquad (8)
\end{aligned}
$$

$$
\begin{aligned}
&(\rho-a_{1R}\varepsilon)(1-a_{2I}\varepsilon)+(1-a_{1I}\varepsilon)(\rho-a_{2R}\varepsilon)\\
&\quad=e^{-1/(a_e\varepsilon)}\{\cos(2\hat{k}_{xR}L_x)[(\rho+a_{1R}\varepsilon)(1+a_{2I}\varepsilon)\\
&\quad\quad +(1+a_{1I}\varepsilon)(\rho+a_{2R}\varepsilon)]\\
&\quad\quad +\sin(2\hat{k}_{xR}L_x)[(\rho+a_{1R}\varepsilon)(\rho+a_{2R}\varepsilon)\\
&\quad\quad -(1+a_{1I}\varepsilon)(1+a_{2I}\varepsilon)]\}. \qquad (9)
\end{aligned}
$$

ρ can be expanded in a perturbation series as

$$\rho=\rho_0+\varepsilon\rho_1+\varepsilon^2\rho_2+\cdots . \qquad (10)$$

Substituting this expansion in Eqs. (8) and (9) and collecting terms of $O(\varepsilon^0)$ yields

$$\rho_0^2=1, \qquad (11)$$

$$\rho_0=0. \qquad (12)$$

As these two equations are contradictory, the assumption must be incorrect, and hence $\hat{k}_{xI}$ is not much larger than $\max\{1/2L_x,|\eta_1 k|,|\eta_2 k|\}$ if $\hat{k}_{xI}\geqslant 0$.

The next theorem shows that when the magnitude of the real part of the eigenvalue is large, the eigenvalue can be roughly estimated (see also Ref. 2).

Theorem 3: *Let $\hat{k}_{xR}$ and $\hat{k}_{xI}$ be the real and imaginary parts of a root of the acoustic eigenvalue equation, respectively. If $|\hat{k}_{xR}|\gg\max\{|\eta_1 k|,|\eta_2 k|\}$, then $|\hat{k}_{xR}|\approx n\pi/L_x$, where n is an integer, and $\hat{k}_{xI}\approx 0$.*

Proof: If $|\hat{k}_{xR}|\gg\max\{|\eta_1 k|,|\eta_2 k|\}$, then a real number ε with $|\varepsilon|\ll 1$ can be introduced to represent $\eta k/\hat{k}_{xR}$ as $\eta_{1R}k/\hat{k}_{xR}=a_{1R}\varepsilon$, $\eta_{1I}k/\hat{k}_{xR}=a_{1I}\varepsilon$, $\eta_{2R}k/\hat{k}_{xR}=a_{2R}\varepsilon$, and $\eta_{2I}k/\hat{k}_{xR}=a_{2I}\varepsilon$, respectively, where $|a|\leqslant 1$. Using the notation $\rho=\hat{k}_{xI}/\hat{k}_{xR}$, the division of Eqs. (6) and (7) by $\hat{k}_{xR}^2$ leads to

$$
\begin{aligned}
&(1-a_{1R}\varepsilon)(1-a_{2R}\varepsilon)-(\rho-a_{1I}\varepsilon)(\rho-a_{2I}\varepsilon)\\
&\quad=e^{-2\hat{k}_{xI}L_x}\{\cos(2\hat{k}_{xR}L_x)[(1+a_{1R}\varepsilon)(1+a_{2R}\varepsilon)\\
&\quad\quad -(\rho+a_{1I}\varepsilon)(\rho+a_{2I}\varepsilon)]\\
&\quad\quad -\sin(2\hat{k}_{xR}L_x)[(1+a_{1R}\varepsilon)(\rho+a_{2I}\varepsilon)\\
&\quad\quad +(\rho+a_{1I}\varepsilon)(1+a_{2R}\varepsilon)]\}, \qquad (13)
\end{aligned}
$$

$$
\begin{aligned}
&(1-a_{1R}\varepsilon)(\rho-a_{2I}\varepsilon)+(\rho-a_{1I}\varepsilon)(1-a_{2R}\varepsilon)\\
&\quad=e^{-2\hat{k}_{xI}L_x}\{\cos(2\hat{k}_{xR}L_x)[(1+a_{1R}\varepsilon)(\rho+a_{2I}\varepsilon)\\
&\quad\quad +(\rho+a_{1I}\varepsilon)(1+a_{2R}\varepsilon)]\\
&\quad\quad +\sin(2\hat{k}_{xR}L_x)[(1+a_{1R}\varepsilon)(1+a_{2R}\varepsilon)\\
&\quad\quad -(\rho+a_{1I}\varepsilon)(\rho+a_{2I}\varepsilon)]\}. \qquad (14)
\end{aligned}
$$

Substituting the perturbation expansion of ρ in Eq. (10) into Eqs. (13) and (14) and focusing on the terms of $O(\varepsilon^0)$ shows that

$$(\rho_0^2-1)[e^{-2\hat{k}_{xI}L_x}\cos(2\hat{k}_{xR}L_x)-1]+2\rho_0 e^{-2\hat{k}_{xI}L_x}\sin(2\hat{k}_{xR}L_x)=0, \tag{15}$$

$$2\rho_0[e^{-2\hat{k}_{xI}L_x}\cos(2\hat{k}_{xR}L_x)-1]-(\rho_0^2-1)e^{-2\hat{k}_{xI}L_x}\sin(2\hat{k}_{xR}L_x)=0. \tag{16}$$

The elimination of ρ_0 reduces these two equations to

$$[e^{-2\hat{k}_{xI}L_x}\cos(2\hat{k}_{xR}L_x)-1]^2+[e^{-2\hat{k}_{xI}L_x}\sin(2\hat{k}_{xR}L_x)]^2=0. \tag{17}$$

This implies that

$$e^{-2\hat{k}_{xI}L_x}\cos(2\hat{k}_{xR}L_x)=1, \tag{18}$$

$$e^{-2\hat{k}_{xI}L_x}\sin(2\hat{k}_{xR}L_x)=0. \tag{19}$$

The solutions of these equations are

$$\hat{k}_{xR}=\frac{n\pi}{L_x}, \tag{20}$$

$$\hat{k}_{xI}=0, \tag{21}$$

where n is an integer. ■

Theorem 3 indicates that if the magnitude of the real part of the solution is large relative to $|\eta_1 k|$ and $|\eta_2 k|$, then it is sufficient to find eigenvalues near $k_x=n\pi/L_x$, which are the eigenvalues when the walls are perfectly rigid both on $x=0$ and $x=L_x$. Therefore, the initial intervals used in the IN/GB method can be small and set only near $k_x=n\pi/L_x$ for large k_{xR}. Alternatively, the classical Newton iterative method can be used for Eq. (5) with the complex variable k_x for $|k_{xR}|\gg|\eta_1 k|,|\eta_2 k|$ with initial guesses $n\pi/L_x$. In either case, the knowledge of the approximate solutions can be used to vastly improve the computational efficiency.

In summary, the region on the complex plane in which the eigenvalues are sought can be restricted as follows:

(1) $0\leqslant k_{xI}$.
(2) k_{xI} is not much larger than $\max\{1/2L_x,|\eta_1 k|,|\eta_2 k|\}$.
(3) Near $k_x=n\pi/L_x$, if $|k_{xR}|\gg|\eta_1 k|,|\eta_2 k|$.

Although the limits and approximations of acoustic eigenvalues are derived to improve the efficiency of the IN/GB implementation, they may be applied to all methods for finding acoustic eigenvalues and are not restricted to the IN/GB method.

In the following sections, three numerical experiments are performed to show the accuracy, efficiency, and the utility of the IN/GB method.

IV. NUMERICAL EXPERIMENT 1: EIGENVALUE CALCULATION

Eigenvalues in the x direction were found by implementing the multivariate IN/GB method for solving the eigenvalue equations [Eqs. (6) and (7)] for driving wave numbers $k=2$, 10, and 20. These wave numbers correspond roughly to the frequencies of 100, 500, and 1000 Hz, respectively. In all calculations, $L_x=1$ m, and the specific acoustic admittances of the walls were set based on Fig. 1 in Ref. 14, which shows the specific acoustic impedances of some commercial acoustic materials with rigid wall backing. At each frequency, the specific impedances of Celotex C-4 1.25 in. and Johns-Manville Acoustex 0.88 in. were obtained from this figure. The impedances of the former material were used at $x=0$ and the latter at $x=1$. Table I shows the specific acoustic impedances used in the calculations. Because typical impedances of commercial materials were used, the resulting boundary conditions represent a real-world situation. Based on Theorems 2 and 3 derived in the previous section, the initial intervals for k_{xI} were set at $[0,10\max\{1/2L_x,|\eta_1 k|,|\eta_2 k|\}]$.

TABLE I. Specific acoustic impedances $Z_1/\rho c$ (on $x=0$) and $Z_2/\rho c$ (on $x=L_x$).

k	$Z_1/\rho c$	$Z_2/\rho c$
2	3.0−16.0 i	3.0−25.0 i
10	2.5−2.0 i	1.5−5.0 i
20	3.0+2.0 i	1.5−2.0 i

The implementation of the IN/GB algorithm requires an interval arithmetic software package. While some compilers support interval arithmetic,[15] public domain software is also available in several programming languages.[16] INTLIB[17] was used to implement interval arithmetic in this study.

The ten eigenvalues with the smallest real parts are shown in Fig. 2 and Table II for each driving wave number k. Results show that there are a few eigenvalues whose imaginary parts are much larger than the others, e.g., the first eigenvalue for $k=2$ and the second eigenvalues for $k=10$ and $k=20$. The magnitudes of the eigenfunctions corresponding to these roots change more rapidly in space than others [see Eq. (4)]. Although such roots are hard to find by some numerical methods,[7] the IN/GB method succeeds in finding them. Note that this method is guaranteed to find all roots

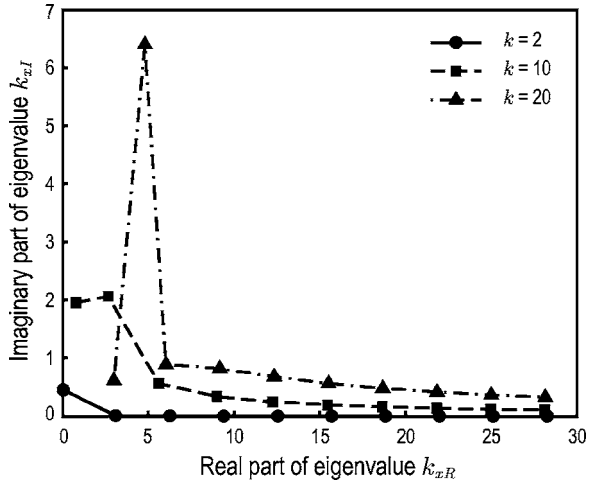

FIG. 2. The ten eigenvalues with the smallest real parts in the x direction with $L_x=1$ m and with boundary impedances shown in Table I.

TABLE II. The ten eigenvalues with the smallest real parts in the x direction with $L_x=1$ m and with boundary impedances shown in Table I.

	$k=2$	$k=10$	$k=20$
1	0.0370+0.4524 i	0.7631+1.9528 i	2.9873+0.6154 i
2	3.0768+0.0106 i	2.6597+2.0652 i	4.8000+6.4000 i
3	6.2513+0.0052 i	5.6177+0.5628 i	6.0268+0.8930 i
4	9.4036+0.0034 i	9.0063+0.3390 i	9.1681+0.8216 i
5	12.5505+0.0026 i	12.2582+0.2467 i	12.3426+0.6812 i
6	15.6952+0.0020 i	15.4635+0.1947 i	15.5169+0.5668 i
7	18.8390+0.0017 i	18.6467+0.1611 i	18.6849+0.4814 i
8	21.9821+0.0015 i	21.8177+0.1375 i	21.8473+0.4171 i
9	25.1248+0.0013 i	24.9813+0.1200 i	25.0053+0.3674 i
10	28.2672+0.0011 i	28.1398+0.1065 i	28.1602+0.3280 i

within a given interval. These results also indicate that it is not appropriate to assume $k_{xR} \gg k_{xI}$, an assumption that has been previously used.[1,2,5]

Whereas Table II and Fig. 2 also validate that the eigenvalues obey the limits and asymptotic behavior derived in Sec. III, these properties are more clearly seen in Fig. 3, which shows the first 1000 eigenvalues ordered by the magnitudes of their real parts. Results show that k_{xI} approaches zero with increasing k_{xR}, as indicated by Theorem 3, and that when k_{xR} is large, the rate of change of k_{xI} with respect to k_{xR} is approximately $O(k_{xR}^{-1})$ for all the driving wave numbers k. The behavior of k_{xR} is shown in more detail in Fig. 4. This figure shows the difference between k_{xlR}, the real part of the lth eigenvalue, and the nearest $n\pi/L_x$. As expected from Theorem 3, k_{xlR} converges to $n\pi/L_x$ as the mode number l grows, and the convergence rate is found to be approximately $O(l^{-1})$ for all driving frequencies.

The efficiency of the IN/GB algorithm is demonstrated by the observation that 1000 eigenvalues were calculated in about 10 s for all the wave numbers mentioned above on a computer with a 2.4 GHz CPU.

V. NUMERICAL EXPERIMENT 2: MODAL SOLUTION

As an application of the eigenvalues obtained using the IN/GB method, the modal solution of the Helmholtz problem

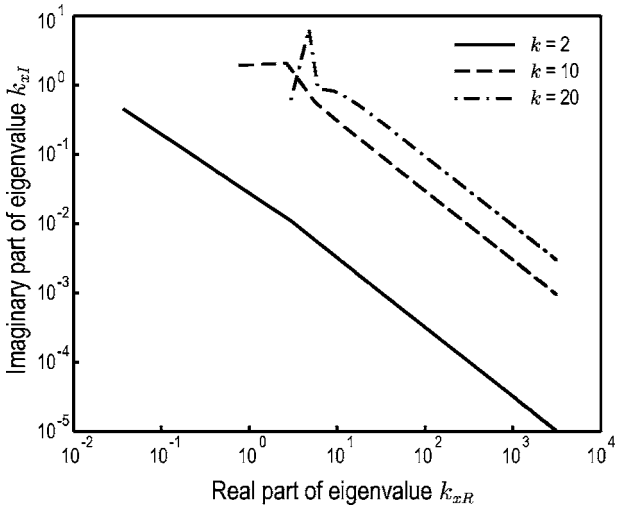

FIG. 3. The 1000 eigenvalues with the smallest real parts in the x direction with $L_x=1$ m and with boundary impedances shown in Table I.

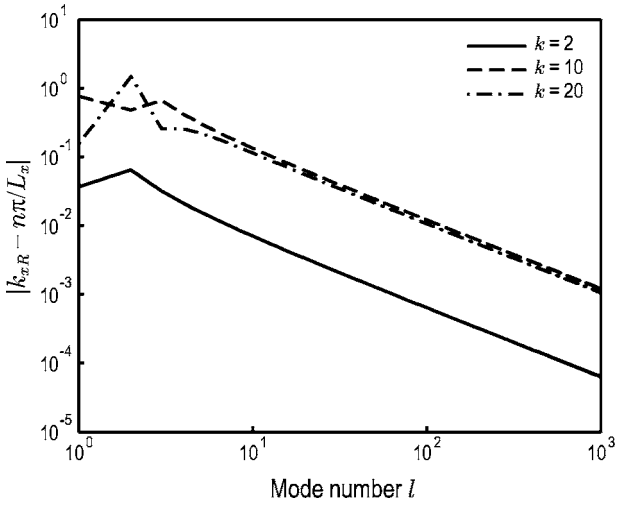

FIG. 4. Difference between the real part of each eigenvalue k_{xR} and the nearest $n\pi/L_x$, which is the eigenvalue when the walls are perfectly rigid.

in a two-dimensional rectangular room is calculated. The modal solution is then compared with the benchmark solution computed using the finite element method (FEM) to discuss the accuracy of the modal solution and hence the validity of the application of the IN/GB approach to the acoustic eigenvalue equation.

The problem domain is the rectangle on the xy plane in Fig. 1, and the size of the room is 1 m $\times$ 1 m (i.e., $L_x=L_y=1$ m). The governing equation is the inhomogeneous Helmholtz equation, given by

$$-\nabla^2 p - k^2 p = \delta(\mathbf{x}-\mathbf{x_s}), \tag{22}$$

in which $\mathbf{x_s}$ is the source position, set at the center of the room, i.e., $\mathbf{x_s}=(x_s,y_s)=(0.5,0.5)$. On the walls at $x=0$ and $x=L_x$, the impedance boundary conditions listed in Table I are imposed for driving wave numbers $k=2,10,20$. The walls on $y=0$ and $y=L_y$ are rigid with a specific acoustic admittance of zero.

A. Modal solution

1. Derivation of modal solution

Once all the eigenvalues in x and y directions are found, the modal solution of Eq. (22) is expressed in the series expansion in terms of the eigenfunctions as

$$p(x,y) = \sum_{l=1}^{\infty}\sum_{m=1}^{\infty} \tilde{A}_{lm}\phi_{xl}(x)\phi_{ym}(y), \tag{23}$$

where $\tilde{A}_{lm}$ are constants to be determined. The lth eigenfunction in the x direction $\phi_{xl}(x)$ is defined by Eq. (4), and similarly for $\phi_{ym}(y)$.

When walls have nonzero acoustic admittance, the eigenfunctions $\phi_{xl}(x)$ are orthogonal in the sense that

$$\int_0^{L_x} \phi_{xl}\phi_{xl'}\,dx = \Lambda_{xl}\delta_{ll'} \quad \text{(no sum on } l\text{)}, \tag{24}$$

where $\delta_{ll'}$ is the Kronecker delta function and

$$\Lambda_{xl} = \int_0^{L_x} \phi_{xl}^2 \, dx \tag{25}$$

$$= 2L_x[k_{xl}^2 - (\eta_1 k)^2] - \frac{i}{2k_{xl}}[(k_{xl} + \eta_1 k)^2(e^{i2k_{xl}L_x} - 1) - (k_{xl} - \eta_1 k)^2(e^{-i2k_{xl}L_x} - 1)]. \tag{26}$$

Note that in Eq. (24), ϕ_{xl} is multiplied by $\phi_{xl'}$, and not by the complex conjugate of $\phi_{xl'}$. This orthogonality can be proven by explicitly evaluating the integral in Eq. (24) and using the fact that k_{xl} satisfy the corresponding acoustic eigenvalue equation, Eq. (5). The eigenfunction is normalized as

$$\psi_{xl}(x) = \frac{\phi_{xl}(x)}{\sqrt{\Lambda_{xl}}}. \tag{27}$$

The modal solution is represented in terms of the orthonormal eigenfunctions as

$$p(x,y) = \sum_{l=1}^{\infty} \sum_{m=1}^{\infty} A_{lm} \psi_{xl}(x) \psi_{ym}(y). \tag{28}$$

A_{lm} are obtained by using the orthogonality of the eigenfunctions, an approach routinely used when the solution is sought for rigid walls. Substituting series expansion, Eq. (28), into the inhomogeneous Helmholtz equation Eq. (22) and making use of the orthonormal property of the eigenfunctions, the modal solution is given by

$$p(x,y) = \sum_{l=1}^{\infty} \sum_{m=1}^{\infty} \frac{1}{k_{lm}^2 - k^2} \psi_{xl}(x) \psi_{ym}(y) \psi_{xl}(x_s) \psi_{ym}(y_s), \tag{29}$$

where k_{lm} are the eigenvalues of the room defined by

$$k_{lm}^2 = k_{xl}^2 + k_{ym}^2. \tag{30}$$

The real parts of k_{lm} correspond to eigenfrequencies or resonance frequencies for the room, while the imaginary parts are the damping constants.[1,5]

Because of the rigid boundary conditions on $y=0$ and $y=L_y$, the eigenfunctions in the y direction are given by [see Eq. (4)]

$$\psi_{ym}(y) = \sqrt{\frac{\epsilon_m}{L_y}} \cos\left(\frac{m\pi}{L_y} y\right), \tag{31}$$

where ϵ_m is the Neumann factor with the value $\epsilon_m = 1$ if $m = 0$ but $\epsilon_m = 2$ if $m \geqslant 1$, and the eigenvalues are given by

$$k_{ym} = m\pi/L_y, \quad m = 0,1,2, \ldots . \tag{32}$$

Substituting these eigenfunctions and eigenvalues into Eq. (29), the modal solution for the entire problem is

$$p(x,y) = \sum_{l=1}^{\infty} \sum_{m=0}^{\infty} \frac{1}{k_{xl}^2 + (m\pi/L_y)^2 - k^2} \times \frac{\epsilon_m}{L_y} \psi_{xl}(x_s) \cos\left(\frac{m\pi}{L_y} y_s\right) \psi_{xl}(x) \cos\left(\frac{m\pi}{L_y} y\right). \tag{33}$$

2. Truncated modal solution

The modal solution is expressed by the infinite series given in Eq. (33); however, in practice, this series is truncated at a finite number of modes. As the truncation criterion, R is introduced such that all normal modes satisfying

$$r_{lm} \equiv |k_{lm}^2 - k^2|^{1/2} \leqslant R \tag{34}$$

are included in the summation. With this criterion, the truncated modal solution is defined as

$$p_R(x,y) = \sum_{\substack{l,m \\ r_{lm} \leqslant R}} \frac{\epsilon_m}{(k_{lm}^2 - k^2) L_y} \psi_{xl}(x_s) \cos\left(\frac{m\pi}{L_y} y_s\right) \psi_{xl}(x) \cos\left(\frac{m\pi}{L_y} y\right). \tag{35}$$

B. Finite element solution

For comparison, the same interior Helmholtz problem was solved using the FEM. In this simulation a uniform mesh of square elements with bilinear interpolations was used. The edge of each square element was 0.002 m long. This corresponded to 1571, 314, and 157 elements per wavelength for $k=2$, 10, and 20, respectively. With this resolution, the finite element solution converges well for all the driving wave numbers considered. Thus, the finite element solution provides a reliable benchmark solution and was used to check the validity of the modal solution.

C. Comparison of modal and finite element solutions

The modal solution was compared with the finite element solution at the nodal points used in the finite element analysis. Nodes inside a square region with a side length of 0.1 m centered at the source position were excluded from the comparison because the analytical solution is unbounded at the source and the finite element solution does not capture this behavior accurately.

The normalized error of the truncated modal solution with respect to the finite element solution is defined by

$$e_R = \sqrt{\frac{\sum_i |p_{\text{fem}}(\mathbf{x_i}) - p_R(\mathbf{x_i})|^2}{\sum_i |p_{\text{fem}}(\mathbf{x_i})|^2}}, \tag{36}$$

where p_{fem} is the finite element solution, and $\mathbf{x_i}$ are the nodal points. As the FEM solution is an accurate approximation of the exact solution, the convergence rate of the normalized error e_R with respect to the truncation criterion R must be the same as that of the analytical truncation error. Figure 5 shows the normalized error e_R as a function of R. The log–log plot shows that for all driving wave numbers k, the error decreases with increasing R with a convergence rate of approximately $O(R^{-1})$. It can be shown that the truncation error for a room with rigid walls also varies as R^{-1}. This observation validates the accuracy of the eigenvalues and the IN/GB method.

The result also strongly supports the assertion that the terms in the summation in Eq. (29) become increasingly less important as $|k_{lm}^2 - k^2|$ increases. Thus, there is an easy-to-

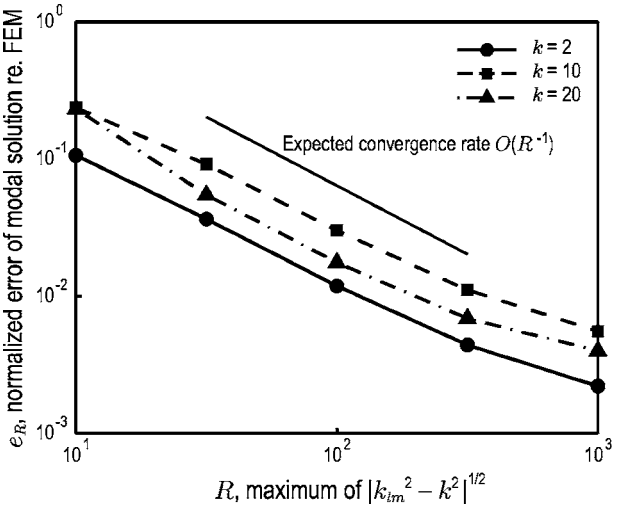

FIG. 5. Normalized difference between the modal solution and the finite element solution with a mesh size of 0.002 m as a function of R, the maximum value of $|k_{lm}^2 - k^2|^{1/2}$ included in the summation used to calculate the modal solution Eq. (35).

evaluate tradeoff between the accuracy of the modal solution and the number of terms included in the summation, and the IN/GB method can be used to find acoustic eigenvalues with whatever precision is desirable or necessary.

VI. NUMERICAL EXPERIMENT 3: ROOM REVERBERATION TIMES

As another example application of finding acoustic eigenvalues using the IN/GB approach, room reverberation times were calculated for three-dimensional rectangular rooms and then compared with the results obtained from the finite-difference time-domain (FDTD) method reported by Yasuda *et al.* in Ref. 13. The width and the depth of the room were L_x=24 m, L_y=12 m, respectively, and the height was either L_z=3 m or L_z=6 m. An absorber with absorption coefficient α=0.5 was installed either only at z=0 or both at z=0 and z=L_z. All other walls were assumed to have α =0.05. The corresponding specific acoustic impedances were all given as real values, i.e.,

$$\frac{Z}{\rho c} = \frac{1 + \sqrt{1-\alpha}}{1 - \sqrt{1-\alpha}}. \tag{37}$$

For these conditions, the reverberation times in 1/3 octave bands were calculated using the eigenvalues obtained by the IN/GB method.

In order to estimate the reverberation times, the collective modal decay curves were first obtained by

$$\langle p^2 \rangle(\Delta f, t) = 10 \log\left(\frac{\sum_{\Delta f} e^{-2k_{\mathbf{N}I}t}/k_{\mathbf{N}I}}{\sum_{\Delta f} 1/k_{\mathbf{N}I}} \right), \quad \text{in dB}, \tag{38}$$

where t is time, $\mathbf{N}$ is a trio of l, m, and n (the mode numbers in the x, y, and z directions, respectively), $k_{\mathbf{N}I}$ is the damping constant (the imaginary part of the eigenvalue $k_{\mathbf{N}}$), and the summation is over all eigenvalues whose eigenfrequencies (real parts of $k_{\mathbf{N}}$) are within the band Δf.[7,18] Although this decay curve is not exact, it roughly characterizes the energy

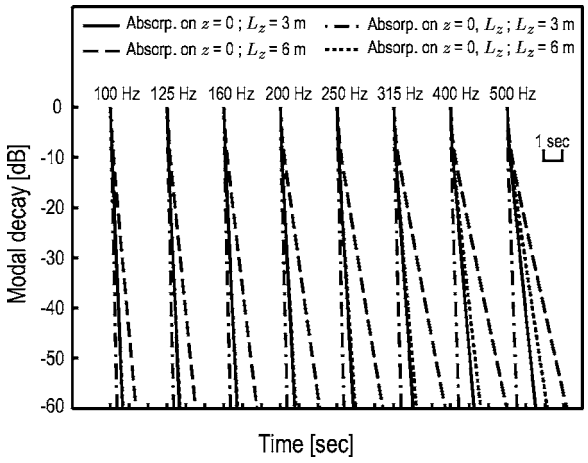

FIG. 6. Collective modal decay curves in 1/3 octave bands of rectangular rooms of size 24 m×12 m×L_z m. The height of the room is either L_z =3 m or 6 m, and an absorbing material is either only on z=0 or both on z=0 and z=L_z.

decay with time in a given frequency band. Figure 6 shows the decay curves obtained from Eq. (38) in 1/3 octave bands for all height and absorber configuration conditions mentioned above. The driving wave numbers k were set such that they correspond to the center frequencies of the 1/3 octave bands.

The reverberation times T_{60} were obtained from the modal decay curve, Fig. 6, and are plotted in Fig. 7 along with the reverberation times computed in Ref. 13, which used the FDTD approach to solve the same problem. A comparison between the room reverberation times using these two approaches shows that all trends are in close agreement. The only major distinction is that the reverberation times using the IN/GB method and decay curve, Eq. (38), are shorter than those found using the FDTD approach. However, the differences are consistent across all frequencies and conditions, and the correlation coefficient between the FDTD and modal decay with the IN/GB method (32 points corresponding to 8 frequency bands and 4 height/absorption con-

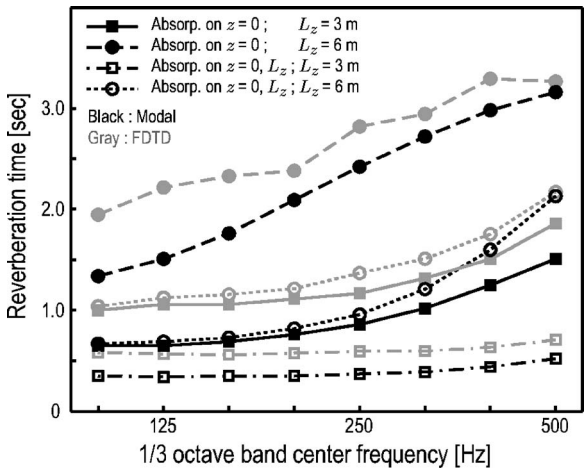

FIG. 7. Reverberation times of rectangular rooms of size 24 m×12 m ×L_z m. The height of the room is either L_z=3 or 6 m, and an absorbing material is either only on z=0 or both on z=0 and z=L_z. Data using the FDTD method were provided by Yasuda *et al.*, taken from their study, Ref. 13.

ditions for each method) is 0.9853. One possible reason for the systematic difference between the values found using the two approaches is that Eq. (38) is an approximation based on averaging the source and receiver positions over the entire room space, while the reverberation times were calculated in Ref. 13 for a specific source/receiver position.

Numerical approaches for finding reverberation times, such as finite element or finite difference methods, are computationally expensive, especially for large rooms or for high frequencies. On the other hand, the computational cost of finding reverberation times based on finding acoustic eigenvalues using the IN/GB method is considerably cheaper than these numerical methods.

VII. CONCLUSIONS

In this study, the IN/GB method was applied to the acoustic eigenvalue equation of a rectangular room with arbitrary, uniform wall impedances to find all eigenvalues within a given interval. Furthermore, the limits and asymptotic behavior of these eigenvalues were derived. These properties were used to restrict the interval range in the IN/GB method and to provide "good" initial guesses, increasing its efficiency in finding all eigenvalues. Several numerical tests were performed to validate the proposed method and to demonstrate its accuracy and efficiency. In the first test, it was verified that the roots obtained using the IN/GB method satisfied the analytical estimates we developed. In the second test, the IN/GB method was used to compute the modal solution corresponding to a point source in a two-dimensional room. This solution was compared with a well-resolved finite element solution, which was used as a benchmark. It was found that as the number of modes in the modal solution are increased, it converged to the FEM solution at the expected analytical rate. Finally, the IN/GB method was used to evaluate the reverberation times for a three-dimensional room with finite wall impedances. These results were compared with the FDTD results obtained by other researchers.[13] It was found that the IN/GB results were in good agreement with the FDTD results.

With the development of interval arithmetic software, it will become increasingly easy to apply the interval method. Therefore, in conjunction with the properties of acoustic eigenvalues derived in this study, the IN/GB method presents an efficient method for solving the acoustic eigenvalue equation for rectangular rooms with arbitrary, uniform wall impedances.

ACKNOWLEDGMENTS

This work was supported by a grant from the Air Force Office of Scientific Research. The authors are very grateful to Yosuke Yasuda, Shinichi Sakamoto, Ayumi Ushiyama, and Hideki Tachibana for their generosity in sharing with us the raw data from their paper, Ref. 13. Dr. Ning Xiang and two anonymous reviewers provided many helpful comments on earlier drafts of this paper.

APPENDIX A: INTERVAL ARITHMETIC

Real interval arithmetic operates on closed, real intervals. Let $X=[\underline{x},\overline{x}]$ denote a real interval with lower limit $\underline{x}$ and upper limit $\overline{x}$, and similarly define as $Y=[\underline{y},\overline{y}]$. The elementary interval operations are defined as follows:[9–12]

$$X+Y=[\underline{x}+\underline{y},\overline{x}+\overline{y}], \tag{A1}$$

$$X-Y=[\underline{x}-\overline{y},\overline{x}-\underline{y}], \tag{A2}$$

$$X\times Y=[\min\{\underline{x}\underline{y},\underline{x}\overline{y},\overline{x}\underline{y},\overline{x}\overline{y}\},\max\{\underline{x}\underline{y},\underline{x}\overline{y},\overline{x}\underline{y},\overline{x}\overline{y}\}], \tag{A3}$$

$$1/X=[1/\overline{x},1/\underline{x}], \quad \text{if } 0\notin X, \tag{A4}$$

$$X/Y=X\times 1/Y. \tag{A5}$$

Note that although the reciprocation $1/X$ or the division Y/X are undefined in ordinary interval arithmetic if $0\in X$, they can be defined in extended arithmetic.[11]

APPENDIX B: INTERVAL EXTENSION OF FUNCTIONS

Elementary functions, such as trigonometric functions and exponentials, can also be extended to work on intervals.[9–11] For a function $f(x):\mathbb{R}\rightarrow\mathbb{R}$, its interval extension $f(X)$ is defined such that

$$\{f(x)|x\in X\}\subseteq f(X). \tag{B1}$$

The definition of the interval extension of a function can also be more intuitively represented as

$$f(X)=[\min_{x\in X} f(x),\max_{x\in X} f(x)]. \tag{B2}$$

APPENDIX C: UNIVARIATE IN/GB METHOD

For a problem with only one variable, the mean value theorem implies

$$f(x)-f(x^*)=(x-x^*)f'(\xi), \tag{C1}$$

for some ξ satisfying $x\leqslant\xi\leqslant x^*$. In Eq. (C1), f' denotes the derivative of f. If x^* is the root of f [i.e., $f(x^*)=0$] and $f'(\xi)\neq 0$, then the root of f can be represented from Eq. (C1) as

$$x^*=x-\frac{f(x)}{f'(\xi)}. \tag{C2}$$

Now let X be an interval such that $x,x^*\in X$, and hence $\xi\in X$. If $f'(X)$ is the interval extension of $f'(x)$ over the interval X, then by definition $f'(\xi)\in f'(X)$. Therefore, the interval arithmetic formulation of Eq. (C2) becomes

$$x^*=x-\frac{f(x)}{f'(\xi)}\in x-\frac{f(x)}{f'(X)}\equiv N(x,X), \tag{C3}$$

where $N(x,X)$ is called the Newton operator. Thus, x^*, the root of f in X, must be in the intersection $X\cap N(x,X)$.

In each iteration step of the interval Newton method, the Newton operator is used to narrow the potential interval containing the roots. The nth iteration of the interval Newton method is defined as follows:

$$x^{(n)} = m(X^{(n)}), \tag{C4}$$

$$N(x^{(n)}, X^{(n)}) = x^{(n)} - \frac{f(x^{(n)})}{f'(X^{(n)})}, \tag{C5}$$

$$X^{(n+1)} = X^{(n)} \cap N(x^{(n)}, X^{(n)}), \tag{C6}$$

where $m(X)$ is the midpoint of X, calculated for $X=[\underline{x}, \overline{x}]$ as

$$m(X) = \frac{\underline{x} + \overline{x}}{2}, \tag{C7}$$

and the number in parentheses in the superscripts denotes the iteration number. The input of the nth step is $X^{(n)}$ and the output is $X^{(n+1)}$.

The number of roots in X is then found from investigating the output interval based on the following properties:

(a) If $X^{(n+1)}=\emptyset$, i.e., if $N(x^{(n)}, X^{(n)}) \cap X^{(n)}=\emptyset$, then there is no root of f in $X^{(n)}$.
(b) If $X^{(n+1)}=N(x^{(n)}, X^{(n)},)$, i.e., if $N(x^{(n)}, X^{(n)}) \subset X^{(n)}$, then f has a unique root in $X^{(n)}$.
(c) If neither (a) nor (b) is satisfied, then more than one root may exist in $X^{(n)}$.

Proofs of these properties can be found in Refs. 9–11 and 19. In case (a), the input interval $X^{(n)}$ can be discarded. In case (b) or (c), the output interval $X^{(n+1)}$ is used as the input of the next step to further narrow the interval.

If $X^{(n)}=X^{(n+1)}$, i.e., if $X^{(n)} \subseteq N(x^{(n)}, X^{(n)})$, then the interval must be bisected. In such a case, the next step of the interval Newton method must be implemented for each of the divided intervals. The natural choice of the bisection point is the midpoint of the interval. When the interval Newton method is combined with this bisection technique, it is called the interval Newton/generalized bisection (IN/GB) method.

The number of roots in $X^{(n)}$ is known if $X^{(n+1)}$ satisfies the conditions of properties (a) or (b). In case (c), although the number of roots in $X^{(n)}$ is unknown, further IN/GB iterations lead all the subintervals of $X^{(n)}$ to either case (a) or (b). Therefore, after a certain number of iterations, it is assured that all subintervals that constitute the entire range of the initial interval have either zero or one root. Hence, once the roots are found in all subintervals in case (b), it is guaranteed that all roots in the initial interval are found.

The termination criteria of the iteration of the IN/GB implementation can be given by the residuals and/or the width of the intervals. Therefore, accuracy of the IN/GB solutions is easily controlled. Once the intervals containing unique roots are sufficiently small, any points inside these intervals can be taken as the approximate roots of the equation. Alternatively, a certain point inside such an interval can be used as the initial guess of a classical method to calculate a closer approximation of the root.

If $0 \in f'(X^{(n)})$, the division on the right-hand side of Eq. (C5) can be evaluated by extended interval arithmetic.[11] In this case, $N(x^{(n)}, X^{(n)})$ may consist of two disjoint, semi-infinite intervals. However, after taking the intersection with the bounded interval $X^{(n)}$ in Eq. (C6), the output of nth iteration $X^{(n+1)}$ is bounded, although it may consist of two intervals. If the output of a certain iteration contains two intervals, the next IN/GB step must be implemented for each interval.

APPENDIX D: MULTIVARIATE IN/GB METHOD

For a problem with r variables, x, X, and f are extended in vector form as

$$\mathbf{x} = [x_1, x_2, \ldots, x_r]^T, \tag{D1}$$

$$\mathbf{X} = [X_1, X_2, \ldots, X_r]^T, \tag{D2}$$

$$\mathbf{f} = [f_1, f_2, \ldots, f_r]^T. \tag{D3}$$

Note that the components of $\mathbf{x}$ and $\mathbf{f}(\mathbf{x})$ are real numbers, while those of $\mathbf{X}$ and $\mathbf{f}(\mathbf{X})$ are real intervals. The simple multivariate extension of the Newton operator becomes

$$\mathbf{N}(\mathbf{x}, \mathbf{X}) = \mathbf{x} - \mathbf{F}'(\mathbf{X})^{-1}\mathbf{f}(\mathbf{x}), \tag{D4}$$

where $\mathbf{F}'(\mathbf{X})$ is the interval extension of the Jacobian matrix of $\mathbf{f}(\mathbf{x})$. Unlike the univariate case, the multivariate Newton operator can be used only when the Jacobian matrix $\mathbf{F}'$ is not singular, i.e., $0 \notin \det\{\mathbf{F}'(\mathbf{X})\}$. If the Jacobian matrix is singular, computations of the matrix-vector product of $\mathbf{F}'(\mathbf{X})^{-1}$ and $\mathbf{f}(\mathbf{x})$ require the addition and/or subtraction of semi-infinite intervals; however, such operations are not defined. For this reason, the Krawczyk operator[9–11] is widely used for multivariate problems instead of the Newton operator.

In the Krawczyk method, the classical multivariate Newton method is treated as a fixed point iteration. The Krawczyk operator can be used even if the interval extension of the Jacobian matrix is singular. This operator is defined as

$$\mathbf{K}(\mathbf{x}, \mathbf{X}) = \mathbf{x} - \mathbf{Y}\mathbf{f}(\mathbf{X}) + [\mathbf{I} - \mathbf{Y}\mathbf{F}'(\mathbf{X})](\mathbf{X} - \mathbf{x}), \tag{D5}$$

where $\mathbf{I}$ is the identity matrix. $\mathbf{Y}$ is an approximation of the inverse of the interval Jacobian matrix and $\mathbf{Y} = \{m[\mathbf{F}'(\mathbf{X})]\}^{-1}$ is frequently used, where m is the midpoint defined by Eq. (C7). The Krawczyk method can be used by extending Eqs. (C4)–(C6) to multivariate form and replacing the Newton operator by the Krawczyk operator.

[1] P. M. Morse and R. H. Bolt, "Sound waves in rooms," Rev. Mod. Phys. **16**, 69–150 (1944).
[2] L. Cremer and H. A. Müller, *Principles and Applications of Room Acoustics*, Vol. **2** (Applied Science Publishers, New York, 1982); english translation by T. J. Schultz.
[3] A. D. Pierce, *Acoustics—An Introduction to Its Physical Principles and Applications* (Acoustical Society of America, New York, 1994).
[4] D. T. Blackstock, *Fundamentals of Physical Acoustics* (Wiley-Interscience, New York, 2000).
[5] H. Kuttruff, *Room Acoustics*, 4th ed. (Spon Press, London, 2000).
[6] P. M. Morse, "The transmission of sound inside pipes," J. Acoust. Soc. Am. **11**, 205–210 (1939).
[7] S. R. Bistafa and J. W. Morrissey, "Numerical solutions of the acoustic eigenvalue equation in the rectangular room with arbitrary (uniform) wall impedances," J. Sound Vib. **263**, 205–218 (2003).
[8] S. L. Hodge, W. E. Zorumski, and W. R. Watson, "Solution of the three-dimensional Helmholtz equation with nonlocal boundary conditions," NASA Technical Memorandum 110174, 1995.
[9] R. E. Moore, *Methods and Applications of Interval Analysis* (SIAM, Philadelphia, 1979).
[10] A. Neumaier, *Interval Methods for Systems of Equations* (Cambridge University Press, Cambridge, 1990).

[11]R. B. Kearfott, *Rigorous Global Search: Continuous Problems* (Kluwer Academic, Dordrecht, 1996).
[12]T. Sunaga, "Theory of an interval algebra and its application to numerical analysis," in *RAAG Memoirs* (Gakujutsu Bunken Fukyu-kai, Tokyo, 1958), Vol. **2**, pp. 29–46 (547–564).
[13]Y. Yasuda, S. Sakamoto, A. Ushiyama, and H. Tachibana, "Reverberation characteristics in a room with unevenly-distributed absorbers: Numerical analysis," Acoust. Sci. Tech. **26**, 388–390 (2005).
[14]L. L. Beranek, "Acoustic impedance of commercial materials and the performance of rectangular rooms with one treated surface," J. Acoust. Soc. Am. **12**, 14–23 (1940).
[15]M. J. Schulte, A. Akkas, V. A. Zelov, and J. C. Burley, "Compiler support for interval arithmetic," in *Proceedings of the 16th IEEE Instrumentation and Measurement Technology Conference*, Venice, Italy, May 1999, pp. 1189–1193.
[16]C. Hu, S. Xu, and X. Yang, "A review on interval computation—Software and applications," Int. J. Comput. Numer. Anal. Appl. **1**, 149–162 (2002).
[17]R. B. Kearfott, M. Dawande, K. Du, and C. Hu, "INTLIB: A portable FORTRAN 77 interval standard-function library," ACM Trans. Math. Softw. **20**, 447–459 (1994).
[18]K. Bodlund, "Monotonic curvature of low frequency decay records in reverberation chambers," J. Sound Vib. **73**, 19–29 (1980).
[19]E. R. Hansen, *Topics in Interval Analysis* (Clarendon, Oxford, 1969).